Complex resistivity decomposition of the Dias's model in partition fractions applied to electrolyte salinity, clay content and hydraulic permeability determination

Alexandre Nunes Barreto (1) and Carlos Alberto Dias (2)
(1) IFF Instituto Federal Fluminense, email: alexandrenunesbarreto@hotmail.com
(2) UENF / LENEP, email: diaslenep@gmail.com

Abstract

In the last years there has been an interest in the induced polarization applied to hydraulic permeability and pore size distribution curve estimation. An electrical model able to describe the complex resistivity behavior in the frequency interval and also provide these attributes is appealing. The complex resistivity function associated to Dias' model to describe the IP phenomenon in rocks has shown a good performance on fitting several experimental data from literature and to identify the physical mechanisms involved in the induced polarization phenomenon, as well as, to determine their *relaxation time*. As a consequence, a new method for determination of the electrolyte salinity, the clay content and the hydraulic permeability based on Dias's model parameters is proposed.

Introduction

The geophysical application of the induced polarization phenomenon and the development of the method (IP) had its first advance in 1946-1955, in the research performed by the group led by A. Brant, at Newmont Exploration Ltd (Brant, 1959). The application of this effect for metallic mineral prospection was then consolidated.

In the period from 1957 to 1959 the understanding of the physical phenomenon in mineralized rocks had a great improvement (Madden and Marshall, 1959a, b ; Marshall and Madden, 1959). These authors developed a thorough analysis of the induced polarization phenomenon in the metal/electrolyte interface (electrode polarization) and ion exchange minerals/electrolyte interface (membrane polarization).

In 1968, an important contribution was given by Dias (1968). This author proposed that in the frequency domain, the rock porous space has a locus where the polarization effect is generated, that incorporates two regions free of polarization: one in series with the metal/electrolyte interface and another totally free in parallel with the first branch of this circuit. This free path in parallel can be in the same pore or in another one in parallel with the first. Dias (1968, 1972, 2000) introduced the concept of total current conductivity and the idea of an electrical behavior cell unity in the bulk of the rock sample. The frequency interval where the induced polarization phenomenon occurs was also determined as 1 mHz to 1 MHz.

In the decades ahead, the induced polarization method was applied also in environmental contamination studies (Vanhala et al, 1992; Borner et al, 1993; Lima and Porsani, 1994; Zonge and Carlson, 1996; Vanhala, 1997) and laboratory measurement for pore size distribution, capilar pressure curve and hydraulic permeability estimation (Olhoeft, 1985; Vinegar and Waxman, 1988; Lima and Niwas, 2000; Kemna et al, 2004; Tong et al, 2004; Tong et al, 2006a, b; Tong and Honggen, 2008; Revil et al. 2012).

The knowledge of the *total current conductivity*, through which is possible to measure the polarization effect, will become in the future an important tool for well log measurement and surface electromagnetic sounding.

The aim of this research is to analyze Dias´s model from its partition fraction decomposition in order to identify the processes occurring on its polarization relaxation.

DIAS's MODEL

According to Dias's model (Dias, 1968; 1972), the first Maxwell equation must include a current density $\vec{J}'$ element associated to internal source as

$$\nabla \mathrm{x}\, \vec{H} = \vec{J}_{oh} + \vec{J}' + \frac{\partial \vec{D}}{\partial t} = \sigma^{\star} \vec{E} \qquad (1)$$

in this way, *the total current conductivity* is given by

$$\sigma^{\star} = \sigma'(\omega) + i\sigma''(\omega) \qquad (2)$$

where $\vec{E}$, $\vec{H}$, $\vec{D}$ are electric, magnetic and electric displacement fields, considering steady state condition and time variation as $e^{i\omega t}$; J_{oh} is the ohmic current density and J' is the current density associated to internal source. The *total current conductivity* is represented by $\sigma^{*}(i\omega)$ and its real and imaginary components given by $\sigma'(\omega)$ and $\sigma''(\omega)$, both real frequency functions. Dias (1968; 1972) proposed the *cell*

unity of the *electrical behavior of rock samples* as shown in the figure 1:

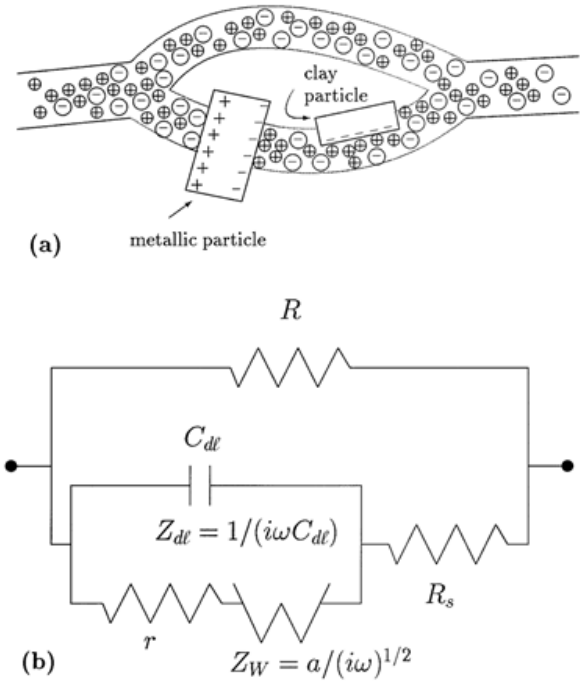

Figure 1: Dias's model for the analog circuit representative of the fundamental cell for the electric behavior of the media under the induced polarization effect: a) Schematic of the low frequency electric polarization in the rocks (IP); b) Fundamental cell of the electric behavior circuit of rocks.

In the analog circuit shown in the figure 1, the impedance $r + Z_W$ represents the induced polarization in the interface generated by diffusion mechanism in series with ohmic conduction and in parallel with capacitive effect (C_{dl}) caused by the electric oscillations of the polarization *locus* as a whole. The inclusion of free pores in series (R_s) and in parallel (R), with the locus where polarization is generated, produces three relaxation times (τ , τ' , τ''). The complex conductivity or resistivity functions, according to Dias´s model, are given by the following equations (3) and (4).

Normalized complex conductivity function

$$\frac{\sigma^* - \sigma_0}{\sigma_0} = \frac{\alpha\beta\lambda(i\omega)^{1/2}}{1 + \beta\lambda'(i\omega)^{1/2}} \qquad (3)$$

where

$$\mu = i\omega\tau\left[1 + \eta(i\omega)^{-1/2}\right] = i\omega\tau + (i\omega\tau'')^{1/2},$$

$$\alpha = m(1-\delta)/(1-m), \quad \beta = (\delta\eta)^{-1},$$

$$\lambda = 1 + \mu, \quad \lambda' = 1 + (1-\delta)\mu.$$

Normalized complex resistivity function

$$\frac{\rho^* - \rho_\infty}{\rho_0} = \frac{m}{1 + i\omega\tau'(1 + 1/\mu)} \qquad (4)$$

where

$$\tau = r C_{dl},$$

$$\tau' = (R + R_s)C_{dl} = [\,(1-\delta)/(1-m)\delta\,]\,\tau,$$

$$\tau'' = (r C_{dl}\,\eta)^2 = (\tau\eta)^2.$$

Parameters description : σ_0 - value of the conductivity at zero frequency, S/m ; ρ_0 - value of the resistivity at zero frequency, Ωm , ($\rho_0 = 1/\sigma_0$) ; m - chargeability, dimensionless ; τ - cell relaxation time due to the induction current generated inside the electrical double layer, s ; τ' - cell relaxation time due to the induction current generated outside the electrical double layer, s ; τ'' - cell relaxation time due to the current generated by diffusion inside the electrical double layer, s ; η - electrochemical parameter, $s^{-1/2}$; δ - cell dimension fraction affected by the polarization, dimensionless.

DECOMPOSITION OF THE DIAS MODEL COMPLEX RESISTIVITY FUNCTION

In the equation (4) it is possible to identify three relaxation times each one related to polarization relaxation of an specific segment of the fundamental cell of the electrical behavior of the rock sample.
The complete decomposition of the complex resistivity can be achieved by the following procedure:

PARTITIAL FRACTIONS DECOMPOSITION
Theoretical formulation

In the equation (4), the function μ is substituted as given in the equation (3). After some algebra and introducing the auxiliary variable $(i\omega)^{1/2} = z$ in the second member of the equation, one obtains

$$\frac{\rho^* - \rho_\infty}{\rho_0} = \frac{\frac{m}{\tau'}(\eta + z)}{\frac{\eta}{\tau'} + \frac{\tau + \tau'}{\tau\tau'}z + \eta z^2 + z^3} \qquad (5)$$

The equation (5) can always be expanded in partition fractions, which going back in the substitution $z = (i\omega)^{1/2}$, results

$$\frac{\rho^{\star}-\rho\infty}{\rho_0}=\frac{m_W}{1+(i\omega\tau_w)^{1/2}}+\frac{m_D}{1+[(i\omega\tau_D)^{1/2}-\nu]^2}+\frac{2m_D\nu[(i\omega\tau_D)^{1/2}-\nu]}{1+[(i\omega\tau_D)^{1/2}-\nu]^2} \quad (6)$$

Where

$\tau_D=\tau\tau'/(\tau+\tau')$; $m_D=m\tau_D/\tau'$;

$\tau_w=(\frac{\tau+\tau'}{\tau})^2/\eta^2$; $m_W=m\tau_D/\tau$;

$\nu=-\frac{1}{2}(1-\frac{\tau_D}{\tau'})\eta\tau_D^{1/2}$; $m_W+m_D=m$.

In the last expression (see experimental results on Table 4) the complete function can be approximated to

$$\frac{\rho^{\star}-\rho\infty}{\rho_0}\simeq\frac{m_W}{1+(i\omega\tau_w)^{1/2}}+\frac{m_D}{1+i\omega\tau_D} \quad (7)$$

Each term in the equation (6) is related to an specific process in the complex resistivity dispersion:
i) the first is associated to the diffusion polarization relaxation in the interface neighborhood, described by a Warburg function, a part chargeability m_W and relaxation time τ_W, which predominates in the low frequency interval ($10^{-3}-10^{2}$ Hz);
ii) the second one is related to a mix of diffusion and induction through the pore in the mid range frequency interval ($10^{2}-10^{4}$ Hz);
iii) the third one is related to the interaction between the double layer capacitance and the free pores regions resistances, described by a Debye function, a part chargeability m_D and a relaxation time τ_D, which predominates in the high frequency interval (10^{4} – 10^{6} Hz);

Relaxation times τ_W, τ_D and factors f_a and f_b

In the expression for τ_W , the relations to τ and τ' as functions of the Dias's model parameters can be introduced, as

$$\tau_w=\left(\frac{\tau+\tau'}{\eta\tau}\right)^2=\left[\frac{1-m\delta}{(1-m)\delta}\right]\frac{1}{\eta^2} \quad (8)$$

or

$$\tau_w=\frac{1}{f_a^2}\frac{1}{\eta^2} \quad (9)$$

where the factor f_a can be defined as

$$f_a=\frac{\tau}{\tau+\tau'}=\frac{(1-m)\delta}{1-m\delta}=\frac{r}{r+R+R_s} \quad (10)$$

The factor f_a incorporates the influence of the relaxation times τ and τ' produced by free pores and its fractions in the interface neighborhood where the polarization occurs.

In the same manner, the relaxation time $\tau_D=\frac{\tau\tau'}{\tau+\tau'}$ can be written as

$$\tau_D=\frac{\tau\tau'}{\tau+\tau'}=(\frac{1-\delta}{1-m\delta})\tau=f_b\tau \quad (11)$$

where

$$f_b=\frac{\tau'}{\tau+\tau'}=\frac{1-\delta}{1-m\delta}=\frac{R+R_s}{r+R+R_s} \quad (12)$$

The factor f_b shows that relaxation time τ_D is directly affected by the relaxation time τ, which by its turn depends on the double layer capacitance. Consequently it is also dependent on the surface area where the electric double layer is formed.
In another way, Chang and Jaffé (1952) obtained experimentally that

$$\eta=\frac{2D_{N_a^+}^{1/2}}{\ell} \quad (13)$$

where $D_{N_a^+}$ is the cation diffusion coefficient given by $1.3\text{x}10^{-9}m^2/s$ (Bockris and Reddy, 1970 - v.1), and ℓ is the electric double layer thickness. Substituting the equation (13) in the equation (9) , one gets

$$\tau_w=\frac{\ell^2}{f_a^2 4D_{N_a^+}} . \quad (14)$$

Assuming that the double layer extension of influence is $\ell \cong d_0/2$, where d_0 is the mineral grain diameter, the equation (14) becomes

$$\tau_w=\frac{d_0^{\,2}}{(2f_a)^2 4D_{N_a^+}} . \quad (15)$$

This is the equation coming from the Dias model interconnecting the relaxation time τ_W with parameters of

the polarization cell and making the bridge to the hydraulic permeability through d_0.

APPLICATION TO EXPERIMENTAL DATA

In order to validate the expressions for the relaxation time τ_W, several experimental data available were selected. The description of these data can be seen on Table 1. The frequency range was extended beyond the experimental data, in order to observe in the curve a second maximum phase peak.
For each data set it is shown in the Appendix A the corresponding Dias's model parameters for complex conductivity (Table 2), complex resistivity (Table 3) and the partition fractions decomposition terms (Table 4).
The values of the parameters obtained for Dias' s model fitting on each experimental data set for complex conductivity were obtained using a software developed by Ribeiro (2010), and the parameters for complex resistivity from its relation to the previous one.
The values of the factors f_a and f_b could then be determined, as well as, τ_W and τ_D, and its relationship to the electrolyte salinity (NaCl) and the clay content (see figure A-1).
It is interesting to observe that the factor f_a has a linear dependence with the electrolyte log concentration, independently of the clay content, as shown by Figure A-1-a. Its relationship to the clay content however has small resolution between 0 and 5% of clay, independently of the electrolyte concentration. It has no variation at high values of electrolyte concentration (1M) in the range 0 to 10% of clay
The best parameters for clay content determination are τ_W and τ_D, as shown by Figures A-1(c, d). The relaxation time τ_W is straightforwardly defined by clay content for electrolyte low concentration (10^{-3}M). However, it is almost independent of clay content when electrolyte concentration is high (1M). The reason for this behavior is the predominance of the pore free conduction when electrolyte concentration is high. The relaxation time τ_D, otherwise, saturates when electrolyte concentration is high (1M) in the interval from 5 to 10% clay content. The parameter τ_D has a maximum value when the clay content is 5% and the electrolyte concentration is low (10^{-3} to 10^{-2} M).
It is possible then to determine from Dias model complex resistivity measurements the electrolyte concentration and the clay content in rock samples (without metallic particles). To do this it is sufficient: (i) to know the mineral composition of the rock sample in order to be sure that there are no metallic particles; (2) to construct the factor f_a curves using the average values shown on Figure A-1(a). It is possible in this way to have a good estimation of the factor f_a by knowing the electrolyte concentration, independently of the clay content. The factor f_a can be determined knowing before the values of the parameters (m and δ) of the Dias's model, when experimental data is fitted with this model; (3) knowing the electrolyte concentration and the factor f_a values, one can estimate clay content using the curves indicated in Figure A-1(b), or determining the relaxation times τ_W or τ_D values using curves of the Figures A-1(c, d).

Table 1: Description of experimental data.

Authors and samples description	
(1) Mahan et al (1986) Sample content: $6,0\%$ calchopyrite radius range: $125-150\mu m$ sand grain diameter:$<53\mu m$ Electrolyte conc.:10^{-3}M (NaCl)	**(6a)** Boadu and Seabrook (2006) Sand grain $+0\%$ clay content Electrolyte concentration: 10^{-3}M (NaCl)
	(6b) Boadu and Seabrook (2006) Sand grain $+0\%$ clay content Electrolyte concentration: 10^{-2}M (NaCl)
(2) Klein and Sill (1982) Sample: glass bead diameter: 40 a $125\mu m$; 10% pyrite and 3% calcium montmorilonite clay 84,4 meq / 100gr Electrolyte conc.:10^{-2}M (NaCl)	**(6c)** Boadu and Seabrook (2006) Sand grain $+0\%$ clay content Electrolyte concentration: 1 M (NaCl)
	(6d) Boadu and Seabrook (2006) Sand grain $+5\%$ clay content Electrolyte concentration: 10^{-3}M (NaCl)
(3) Wong (1979) Sample with $6,3\%$ calchopyrite grains diameter range: 200 to $300\mu m$ (Grisseman (1971) - amostra 798) Electrolyte conc.:10^{-3}M (NaCl)	**(6e)** Boadu and Seabrook (2006) Sand grain $+5\%$ clay content Electrolyte concentration: 10^{-2}M (NaCl)
	(6f) Boadu and Seabrook (2006) Sand grain $+5\%$ clay content Electrolyte concentration: 1 M (NaCl)
(4) Nordsiek and Weller (2008) Samples produced from testimony Location: Harz mountain in Germany Electrolyte conc.: 10^{-3}M (NaCl)	**(6g)** Boadu and Seabrook (2006) Sand grain $+10\%$ clay content Electrolyte concentration: 10^{-3}M (NaCl)
	(6h) Boadu and Seabrook (2006) Sand grain $+10\%$ clay content Electrolyte concentration: 10^{-2}M (NaCl)
(5) Binley et al (2005) Testimony sample VEC7-5 sandstone Location: Sherwood in Eggborough Electrolyte conc.:10^{-2}M (NaCl)	**(6j)** Boadu and Seabrook (2006) Sand grain $+10\%$ clay content Electrolyte concentration: 1 M (NaCl)

Partition fractions decomposition – Illustrative examples

Just a few examples are described here.

Mahan et al (1986) - Case (1) Table 1
The complete and the approximated functions are

$$\frac{\rho^{\star}-69.1}{323} \simeq \frac{0.298}{1+(i\omega\ 7.21\times10^{-3})^{1/2}} + \frac{0.488\ [\,1-4.5\times10^{-6}((i\omega\ 0.388)^{1/2}+2.20)\,]}{1+((i\omega\ 0.388)^{1/2}+2.20)^{2}\times10^{-6}} \quad (16)$$

and

$$\frac{\rho^{\star}-69.1}{323} \simeq \frac{0.298}{1+(i\omega\ 7.21\times10^{-3})^{1/2}} + \frac{0.488}{1+i\omega\ 0.388\times10^{-6}} \quad (17)$$

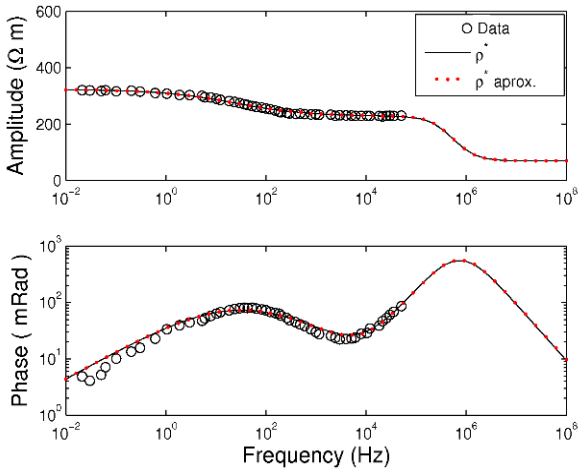

Figure 2: Recomposition of the complex resistivity function in amplitude |ρ| and phase φ of the Dias´s model, applying its partition fractions decomposition for Mahan et al (1986) data - Case (1) Table 1. Theoretical curves extended frequency interval from 10^5 to 10^8 Hz.

Boadu and Seabrook (2006) - Case (6b) Table 1

The complete and the approximated functions are

$$\frac{\rho^{\star}-33.0}{39.8} \simeq \frac{7.26\times10^{-2}}{1+(i\omega\ 2.33\times10^{-4}\ )^{1/2}} + \frac{9.79\times10^{-2}\ [\,1-8.99\times10^{-5}((i\omega\ 3.35)^{1/2}+45.5)\,]}{1+((i\omega\ 3.35)^{1/2}+45.5)^{2}\times10^{-6}} \quad (18)$$

and

$$\frac{\rho^{\star}-33.0}{39.8} = \frac{7.26\times10^{-2}}{1+(i\omega\ 2.33\times10^{-4})^{1/2}} + \frac{9.79\times10^{-2}}{1+i\omega\ 3.35\times10^{-6}} \quad (19)$$

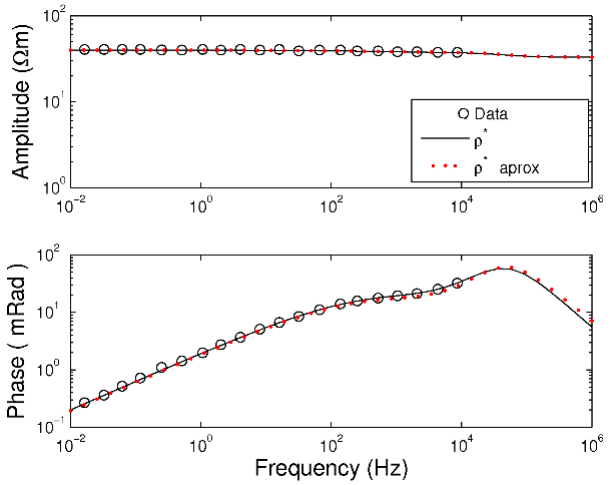

Figure 3: Recomposition of the complex resistivity function in amplitude |ρ| and phase φ of the Dias´s model, applying its partition fractions decomposition for Boadu and Seabrook (2006) data - Case (6b) Table 1. Theoretical curves extended frequency interval from 10^4 to 10^6 Hz.

Based on the results obtained for the complete experimental data set used as reference here, it is possible to confirm that the coefficient ν produces a minor discrepancy in the value of the approximated function compared to the complete function of the complex resistivity, for frequency values lower than 100 kHz.

In general, the complex resistivity $\rho^{\text{å}}$ is described by three processes of dispersion, each one with the respective chargeability and relaxation time. For frequency lower than 100 kHz, the phenomenon can be approximated to two basic dispersion processes of polarization, one generated by diffusion and another by induction.

HYDRAULIC PERMEABILITY ESTIMATION FROM IP

The method proposed by Revil and Florsch (2010) for hydraulic permeability estimation is developed in two steps: (1) mineral grain diameter calculation d_0, using the relation with relaxation time of the cation diffusion in the solution τ_W, given by equation (20); (2) introduction of d_0 into equation (21).

$$\tau_w = \frac{d_0^{\,2}}{8D_{N_a^+}} \quad (20)$$

$$k = \frac{d_0^{\,2}}{32m^2(\mathrm{F}-1)^2\ \mathrm{F}\times0.987\times10^{-15}} \quad (21)$$

Where m = 2 (cimentation fator), $F = \phi^{-m}$ (Formation fator), d_0 (mineral grain diameter in μm) and k (hydraulic permeability in mDarcy).

We are going to substitute the expression (20) by its similar obtained from the Dias model, given by the expression (15)

We intend to use the values of τ_W calculated by Tong et al (2006a) and the experimental values provided by such authors for the hydraulic permeability. For that purpose, let us consider the electrolyte concentration of 0.086 M used by these authors, which corresponds to $f_a \approx 0.42$ through the Figure A-1 (a).

The results shown by Figure A-2 evidenciate that the modification of the Revil and Florsch formula by substitution of equation (20) by the (15) produced estimation values with a coefficient error R = 3.16, smaller than the one (3.91) obtained by Revil and Florsch (2010).

The used error coefficient function, taken from Tong et al. (2006a), is given by

$$[\ln(\mathrm{R})]^2 = \frac{1}{N}\sum_{i=1}^{N}[\ln(\kappa_M(i)) - \ln(\kappa_E(i))]^2 \qquad (22)$$

where k_M is the measured and k_E is the estimated value of permeability.

In this research, it was not possible to have for the experimental data obtained by Tong et al (2006a) the corresponding measurements of the amplitude and phase of the complex resistivity, in order to have the Dias's model specific parameters for these data. Consequently this exercise must be seen only as good enough to show the great potentiality of the Dias model for the hydraulic permeability estimation.

CONCLUSIONS

1. The decomposition of the Dias's model complex resistivity in partition fractions has been done showing the characteristic polarization processes and its respective relaxation times.

2. Three dispersion processes have been identified :

i) the first one is a diffusion-produced polarization in the metal (or clay)-saline solution interface neighborhood, described by a Warburg function, a part chargeability m_W and a relaxation time τ_W. It predominates in the low frequency range (10^{-3} to 10^2 Hz);

ii) the second one relates to a polarization produced by a mix of diffusion and induction of charged particles through the electrical double layer region. It predominates in the frequency mid range (10^2 to 10^4 Hz);

iii) the third one relates to the polarization produced by interaction between the double layer capacitance and the resistances of the free pore regions that take part in the unit cell. It is described by a Debye function and predominates in the high frequency range of the phenomenon (10^4 to 1 MHz);

3. This decomposition was applied to several experimental data available in the literature. It was possible to verify the good performance of the Dias model to describe experimental data and to identify the characteristic frequencies of the phase peaks and the respective polarization relaxation times.

4. Applied to Boadu and Seabrook (2006) experimental data, this procedure provided through the Dias model a new methodology to determine the electrolyte concentration and the clay content in rocks samples without disseminated metallics.

5. Adopting the procedure proposed by Revil and Florsch (2010) for hydraulic permeability estimation, but introducing Dias model parameters, it was possible to improve the results obtained by Revil and Florsch. These authors produced results with an error coefficient R=3.91, while the results obtained with the modified formula had R=3.16. For permeabilities above 10 mDarcy the modified formula reached a value R=1.96, very close of the R=1.76 obtained by Tong et al. (2006a).

ACKNOWLEDGMENTS

The authors acknowledge the North Fluminense State University Campus of Macaé/RJ - Petroleum Exploration and Engineering Laboratory, for providing working facilities for this research and CENPES/PETROBRAS – CARMOD Network, for the financial support to the project through the contracts TC-0050.0061268.10.9 and TC-0050.0066876.11.9. Also thank to CAPES for the PVNS/UFPA fellowship to the second author.

Appendix A

Table 2: Complex conductivity parameter.

Author	σ_o (mS/m)	m	τ (μs)	δ	η $(s^{-1/2})$
(1)	3.09	0.786	1.02	0.884	19.0
(2)	97.1	0.088	243	0.171	10.5
(3)	7.30	0.891	0.109	0.955	20.8
(4)	10.2	0.260	0.100	0.569	14.3
(5)	21.9	0.112	457	0.178	11.4
(6a)	3.40	0.650	43.0	0.880	3.40
(6b)	25.1	0.171	7.60	0.610	116
(6c)	526	0.263	37.0	0.300	71.0
(6d)	48.3	0.170	63.0	0.750	31.0
(6e)	65.8	0.150	46.0	0.640	67.0
(6f)	769	0.050	13.0	0.280	68.0
(6g)	294	0.230	9.0	0.870	125
(6h)	454	0.070	3.5	0.500	30.0
(6j)	833	0.040	14.0	0.280	69.0

Table 3: Complex resistivity parameters.

Author	ρ_o (Ωm)	m	τ (μs)	τ' (μs)	τ'' (μs)
(1)	323	0.786	1.02	0.625	3.76×10^{-4}
(2)	10.3	0.089	243	1197.0	6.51
(3)	137	0.890	0.109	0.0467	5.14×10^{-6}
(4)	97.9	0.260	0.100	0.102	2.05×10^{-6}
(5)	45.7	0.112	457	2370.0	27.14
(6a)	294	0.650	43.0	16.7	21.4×10^{-3}
(6b)	39.8	0.171	7.60	5.85	0.777
(6c)	1.90	0.263	37.0	117.0	6.90
(6d)	20.7	0.170	63.0	25.3	3.81
(6e)	15.2	0.150	46.0	30.5	9.50
(6f)	1.30	0.050	13.0	35.2	0.781
(6g)	3.40	0.230	9.00	1.75	1.26
(6h)	2.20	0.070	3.50	3.76	0.011
(6j)	1.20	0.040	14.0	37.5	0.933

Table 4: Partitial fractions decomposition of the complex resistivity.

Author	m_W	τ_W (ms)	m_D	τ_D (μs)	ν ($\times 10^{-3}$)
(1)	0.298	7.21	0.487	0.388	- 2.2
(2)	0.074	376	0.015	201	- 57.3
(3)	0.267	4.71	0.623	0.0327	- 0.56
(4)	0.131	20.0	0.128	0.0506	- 0.81
(5)	0.094	291	0.018	389.34	- 94.3
(6a)	0.182	167	0.468	12.05	- 1.6
(6b)	0.073	0.23	0.098	3.35	- 45.5
(6c)	0.199	3.24	0.064	29.4	- 145.0
(6d)	0.048	2.02	0.122	18.1	- 18.7
(6e)	0.057	0.59	0.093	18.7	- 56.0
(6f)	0.037	2.92	0.013	9.6	- 76.0
(6g)	0.036	0.091	0.194	1.5	- 12.1
(6h)	0.036	4.78	0.034	1.8	- 10.5
(6j)	0.029	2.78	0.011	10.4	- 80.6

Table 5: Values of τ_W , d_o , f_a and δ obtained from experimental data listed on Table 1.

Author	τ_W (ms)	d_o (μm)	f_a	δ
(1) Mahan (1986)	7.2	4.4	0.62	0.88
(2) Klein and Sill (1982)	378.4	41.0	0.17	0.17
(3) Wong (1979)	4.7	3.6	0.70	0.95
(4) Nordsiek (2008)	6.8	130.7	0.12	0.57
(5) Binley (2005)	295.3	35.6	0.16	0.18
(6a) Boadu and Seabrook (2006)	167.0	24.0	0.72	0.88
(6b) Boadu and Seabrook (2006)	0.2	1.0	0.56	0.61
(6c) Boadu and Seabrook (2006)	3.4	3.4	0.24	0.30
(6d) Boadu and Seabrook (2006)	2.0	3.1	0.71	0.75
(6e) Boadu and Seabrook (2006)	0.6	1.7	0.60	0.64
(6f) Boadu and Seabrook (2006)	3.0	3.8	0.27	0.28
(6g) Boadu and Seabrook (2006)	0.1	0.7	0.84	0.87
(6h) Boadu and Seabrook (2006)	4.8	4.8	0.48	0.50
(6j) Boadu and Seabrook (2006)	2.8	3.7	0.27	0.28

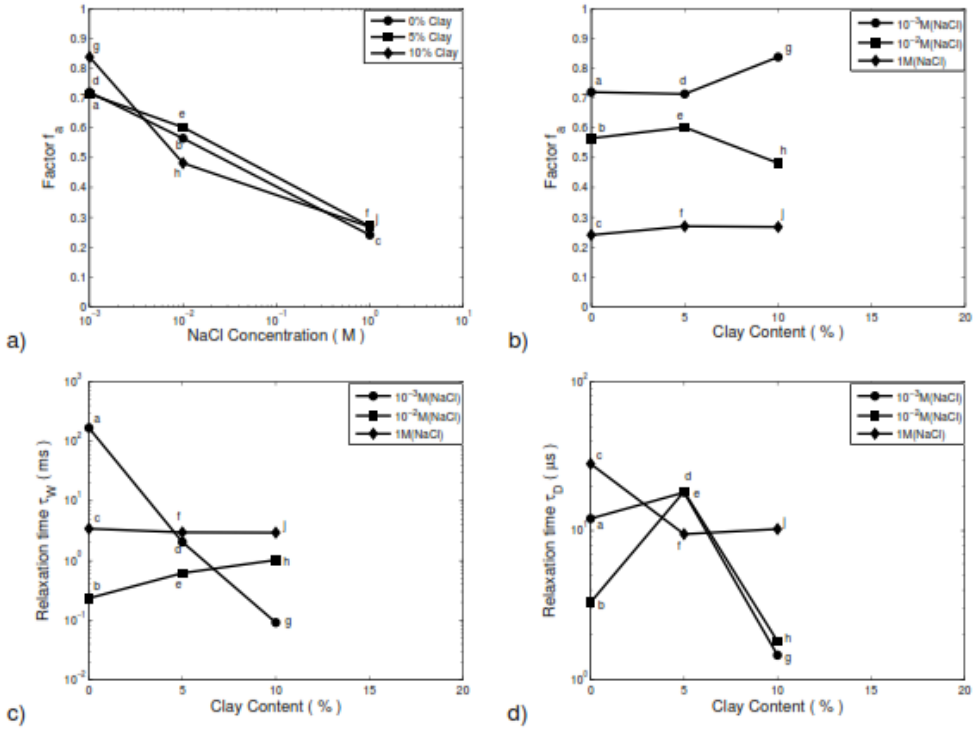

Figure A-1 : Salinity concentration (NaCl) and clay content (% in volume) relationships with the parameters : $f_a = \delta(1-m)/(1-m\delta)$ and the relaxation times τ_W and τ_D, based on data from Boadu and Seabrook (2006) – cases 6(a) until 6(j) / Table 1. (a) and (b), f_a versus concentration and clay content, respectively; (c) and (d), τ_W and τ_D versus clay content, respectively.

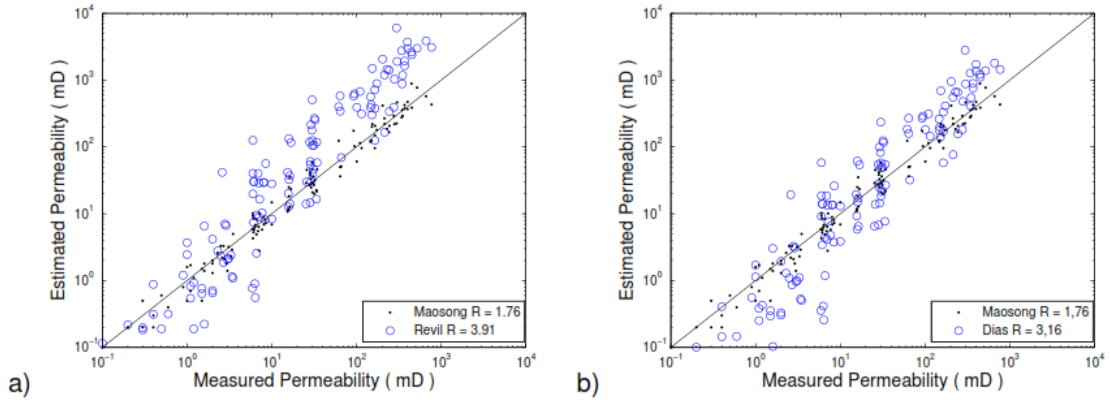

Figure A-2 : Comparative values of hydraulic permeability estimations : (a) by Tong et al. (2006_a – Fig. 4c) and Revil and Florsch (2010 – Fig. 6). (b) by Tong et al. (2006_a – Fig. 4c) and modified Revil and Florsch by Dias model.

REFERENCES

1. Binley, A., Slater, L. D., Fukes, M., and Cassiani, G., 2005, Relationship between spectral induced

polarization and hydraulic properties of saturated and unsaturated sandstone: Water Resources Res., **41**, W12417 / 1-13.

2. Boadu, F. K., and Seabrook, B. C., 2006, Effects of clay content and salinity on the spectral electrical response of soils: Journal of Environmental and Engineering Geophysics, **11**, 161-170.
3. Bockris, J. O'M., and Reddy, A. K. N., 1970, Modern Electrochemistry - vs. 1, 2, Plenum Press.
4. Borner, F., Gruhne, M., and Schon,J., 1993, Contaminations indications derived from electrical properties in the low frequency range: Geophys. Prosp., **41**, 83-98.
5. Brant, A. A., 1959, Historical summary of overvoltage developments by Newmont Exploration Limited 1946–1955, *in* Wait, J. R., Ed., Overvoltage research and geophysical applications: Pergamon Press , Internat. Series on Earth Sciences, **4**, 1-3.
6. Chang, H.C., and Jaffé, G., 1952, Polarization in electrolytic solutions, Part I – Theory: J. Chem. Phys., **20**, 1071–1077.
7. Dias, C. A., and BNDE, 1973, Non-grounded method of geophysical exploration. Canadian Patent n° 920.660.
8. Dias, C. A., 1968, A non-grounded method for measuring electrical induced polarization and conductivity: Ph.D. Thesis, Univ. of California-Berkeley, USA, 260 pp. Link: https://docs.google.com/file/d/0B_nbz7JNT2P9cnZoMmQ5TG1fejQ/edit.
9. ——1972, Analytical model for a polarizable medium at radio and lower frequencies: J. Geophys. Res., **77**, 4945-4956.
10. —— 2000, Developments in a model to describe low frequency electrical polarization of rocks: Geophysics, **65**, 437-451.
11. Kemna, A., Binley, A., and Slater, L., 2004, Crosshole IP imaging for engineering and environmental applications: Geophysics, **69**, 97-107.
12. Klein, J. D., and Sill, W. R., 1982, Electrical properties of artificial clay-bearing sandstones: Geophysics, **47**, 1593-1605.
13. Lima, O. A. L., and Niwas, S., 2000, Estimation of hydraulic parameters of shaly sandstone aquifers from geoelectrical measurements: J. Hydrol. **235**, 12-26.
14. Lima, O. A. L., and Porsani, M. J., 1994, Geo-electrical monitoring of aquifer contamination in the Petrochemical Complex of Camaçari – Bahia: Revista Brasileira de Geofísica, **12**, 147-161 [in Portuguese].
15. Madden, T. R., and Marshall, D. J., 1959a, Electrode and membrane polarization: MIT Report to US Atomic Energy Comm., RME-3157.
16. ———1959b, Induced polarization, a study of its causes and magnitudes in geologic materials: MIT Report to US Atomic Energy Comm., RME-3169.
17. Mahan, M. K., Redman, J. D., and Strangway, D. W., 1986, Complex resistivity of synthetic sulphide bearing rocks: Geophys. Prosp., **34**, 743-768.
18. Marshall, D. J., and Madden, T. R., 1959, Induced polarization - A study of its causes: Geophysics, **24**, 790-816.
19. Nordsiek, S., and Weller, A., 2008, A new approach to fitting induced-polarization spectra: Geophysics, **73**, F235-F245.
20. Olhoeft, G. R., 1985, Low frequency electrical properties: Geophysics, **50**, 2492-2503.
21. Revil, A., and Florsch, N., 2010, Determination of permeability from spectral induced polarization in granular media: Geophys. J. Int., **181**, 1480-1498.
22. Revil A., Koch, K. and Holliger, K., 2012, Relating the permeability of quartz sands to their grain size and spectral induced polarization characteristics, Geophys. J. Int, **190**, 230-242.
23. Ribeiro, E. S., 2010, An efficient strategy for inversion of the complex total current conductivity function of rocks used in the Dias model: MSc dissertation, North Fluminense State Univ. – LENEP/UENF [in Portuguese].Link:https://docs.google.com/file/d/0B_nbz7JNT2P9VFJy WWt3M3dwNmM/edit).
24. Tong, M.., Wang, W., Li, L., Jiang, Y., and Shi, D., 2004, Estimation of permeability of shaly sand reservoir from induced polarization relaxation time spectra: Journal of Petroleum Science and Engineering, **45**, I-10.

25.Tong, M., Li, L., Wang, W., and Jiang, Y., 2006a, A time domain induced- polarization method for estimating permeability in a shaly sand reservoir: Geophys. Prosp., **54**, 623-631.

26.Tong, M., Li, L., Wang, W., and Jiang, Y., 2006b, Determining capillary-pressure curve, pore-size distribution and permeability from induced polarization of shaley sand: Geophysics, **71**, N33-N40.

27.Tong, M., and Tao, H., 2008, Permeability estimating from complex resistivity measurement of shaly sand reservoir: Geophys. J. Int., **173**, 733–739.

28.Vanhala, H., 1997, Mapping oil contaminated sand and till with spectral induced polarization (SIP) method. Geophys. Prosp., **45**, 303-326.

29. Vanhala, H., Soininem, H., and Kukkonem, I., 1992, Detecting organic chemical contaminants by spectral induced polarization method in glacial till environment: Geophysics, **57**, 1014-1017.

30.Vinegar, H. J., and Waxman, M. H., 1988, In situ induced polarization method for determining formation permeability: US Patent Nr 4743854.

31.Wong, J., 1979, An electrochemical model of the induced polarization phenomenon in disseminated sulfide ores, Geophysics, **44**, 1245-1265.

32.Zonge, K. L., and Carlson, N., 1996, Induced polarization effects associated with hydrocarbon accumulations: minimization and evaluation of cultural influences, *in* D. Schumacher and M. A. Abrams, Eds., Hydrocarbon migration and its near-surface expression: AAPG Memoir, **66**, 127 - 137.